

Magnetic-dielectric properties of $\text{NiFe}_2\text{O}_4/\text{PZT}$ particulate composites

This content has been downloaded from IOPscience. Please scroll down to see the full text.

2004 J. Phys. D: Appl. Phys. 37 823

(<http://iopscience.iop.org/0022-3727/37/6/002>)

View [the table of contents for this issue](#), or go to the [journal homepage](#) for more

Download details:

IP Address: 128.125.53.132

This content was downloaded on 08/07/2014 at 23:49

Please note that [terms and conditions apply](#).

Magnetic-dielectric properties of NiFe₂O₄/PZT particulate composites

Junyi Zhai, Ning Cai, Zhan Shi, Yuanhua Lin and Ce-Wen Nan¹

State Key Lab of New Ceramics and Fine Processing, and Department of Materials Science and Engineering, Tsinghua University, Beijing 100084, People's Republic of China

E-mail: cwnan@tsinghua.edu.cn

Received 16 October 2003

Published 24 February 2004

Online at stacks.iop.org/JPhysD/37/823 (DOI: 10.1088/0022-3727/37/6/002)

Abstract

Particulate composites of lead–zirconate–titanate (PZT) and NiFe₂O₄ were prepared using conventional ceramic processing. The measured magnetoelectric (ME) response demonstrated strong dependence on the volume fraction of NiFe₂O₄, the magnetic field, and the angle between the magnetic field and polarization in the ceramics. A large ME voltage coefficient of about 80 mV cm⁻¹ Oe⁻¹ was observed for 0.32NiFe₂O₄/0.68PZT composite ceramic. In particular, at low magnetic fields, the ceramics were found to have a large ME response, linearly varying with both dc and ac magnetic fields.

1. Introduction

The magnetoelectric (ME) effect is defined as an induced dielectric polarization of a material in an applied magnetic field and/or an induced magnetization in an external electric field. ME materials can be used as magnetic sensors for dc or ac magnetic field measurements, transducers or actuators [1–5]. The ME effect was first observed in antiferromagnetic Cr₂O₃ in 1961 [6, 7], and later some single phase crystal families were found to show the ME effect [1]. However, these single-phase materials show such a weak ME effect that they have not yet found any technological applications. Alternatively, piezoelectric/ferrite (e.g. BaTiO₃/CoFe₂O₄) composite ceramics were reported to exhibit a larger ME effect than those of the single-phase materials [8, 9], which resulted from the magnetic–mechanical–electrical interaction between the piezoelectric and ferrite phases. As far as theory is concerned, Harshe [9] and Nan [10], respectively, proposed the first simplified approximation and the first rigorous method to calculate the effective ME properties of such piezoelectric/ferrite ceramic composites. Since then, many researchers have investigated the ME coupling behaviour in the piezoelectric/ferrite composites both experimentally [11–17] and theoretically [18–22].

So far two kinds of ceramic composites have been proposed. One is a particulate ceramic composite of piezoelectric ceramics (such as BaTiO₃ and lead–zirconate–titanate (PZT)) and ferrites. The other is a laminated

composite (e.g. bilayer or multilayer). Most of the studies on such piezoelectric/ferrite ceramic composites [8, 9, 11–17] have mainly focused on their maximum ME coefficient. In this paper, we report simple particulate NiFe₂O₄/PZT composite ceramics. The principal motivation is to investigate the overall coupled magnetic–dielectric properties of such simple particulate composite ceramics.

2. Experimental

Simple NiFe₂O₄ (NFO) was selected as the ferrite due to its cheap and easy availability. NiFe₂O₄ powder with a particle size of about 50 nm was synthesized by a sol–gel method [17], and PbZr_{0.57}Ti_{0.43}O₃ (PZT) was prepared via a conventional solid-state reaction method and its particle size was about 5 μm. NiFe₂O₄ and PZT powders were mixed by a ball milling. The mixtures of f NiFe₂O₄/(1– f) PZT with various volume fractions f were pressed into pellets of around 2 mm in thickness and 10 mm in diameter at 10 MPa. The specimens were finally sintered at 1150°C for 2 h. X-ray diffraction (XRD) and scanning electron microscopy (SEM) were used to reveal the microstructure and phase compositions of the ceramic composites.

In order to make the electrical measurement, the samples were poled at an electric field of 1–3 kV mm⁻¹ at 80°C for about 20 min. The dielectric constants of the specimens were measured using HP4194A LCR. The piezoelectric constant d_{33} was measured by a standard piezo d_{33} meter.

¹ Author to whom any correspondence should be addressed.

The ME effect was obtained by applying an ac magnetic field superimposed on a dc magnetic field on the sample, and then measuring the output charge signal by a dynamic measurement method. An electromagnet was used to provide a dc magnetic field of up to 0.5 T (5 kOe). A teslameter was used to measure the dc magnetic field. A signal generator was used to drive the Helmholtz coil to generate an ac magnetic field of 2 Oe with various frequencies. The charge generated from the sample was measured by a charge amplifier. The output signal from the charge amplifier was measured with a digital oscilloscope. The sample holder can be rotated to change its direction with respect to the applied field, which allows us to investigate the ME anisotropy of the samples. All measurements were made at room temperature.

3. Results and discussion

3.1. Microstructure

Figure 1 shows XRD patterns of the NFO/PZT particulate composites, pure PZT and NFO. All diffraction peaks in the XRD patterns of NFO and PZT can be readily indexed to NFO and PZT, respectively. Basically, the diffraction peaks, except the peak at 28° for the NFO/PZT composites, consist of those of NFO and PZT. The additional peak at 28° corresponds to a new phase rather than NFO and PZT, though it is difficult to determine what phase it is. This additional diffraction peak means that there occurred some reaction (e.g. forming some solid solution) between NFO and PZT when a small amount of NFO was added to PZT. But the additional peak gradually disappears with increase in the concentration of NFO. A typical SEM image shown in figure 2 shows the two different phases distinctly: i.e. grey for PZT and dark for NFO, indicating that NFO and PZT are randomly mixed together.

3.2. Dielectric and piezoelectric constants

Figure 3 shows the dielectric constant ϵ_{33} of the NFO/PZT particulate composite ceramics. PZT is a high-permittivity dielectric material, while the ferrite has a low dielectric constant. As expected, the dielectric constant of the particulate composites decreases with increase in the volume fraction f of NFO (figure 3(a)). But the dielectric constant of the composite sample with $f = 0.07$ shows a large decrease (i.e. about 50% drop) with respect to that of the pure PZT ceramic,

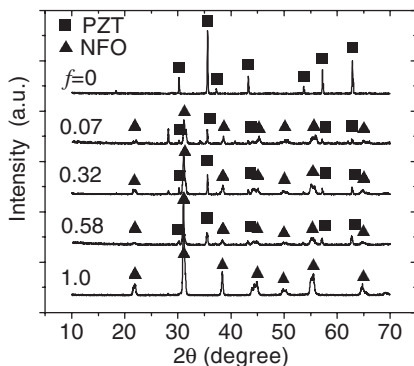


Figure 1. XRD patterns of the NFO/PZT composites, pure PZT and NFO.

which might be due to the reaction between NFO and PZT when a small amount of NFO was added to PZT, as shown in figure 1. The dielectric constants of the composites show weak dependence on the frequency below 10^5 Hz (figure 3(b)), and a large change at around 300 kHz, especially for pure PZT. This change corresponds to the thickness electromechanical resonance for such disc-shaped PZT samples [23].

Figure 4 shows the piezoelectric constant d_{33} for the particulate composite ceramics. As expected, the piezoelectric constant of the ceramics decreases with increase in the volume fraction f of NFO, similar to the dielectric constant

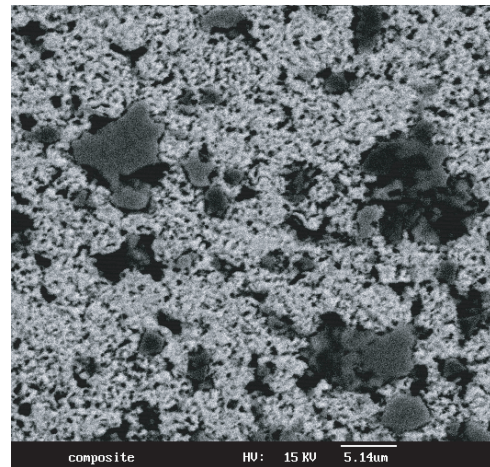


Figure 2. A typical SEM micrograph of the composite with $f = 0.32$.

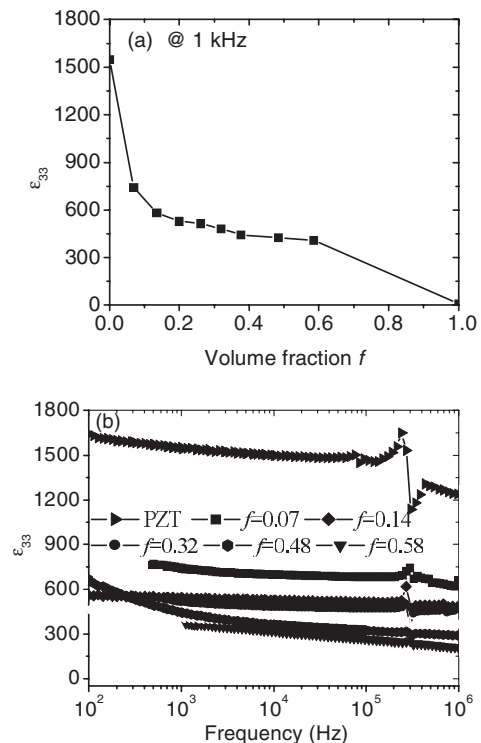


Figure 3. (a) The dielectric constant of the ceramics as a function of the volume fraction f of NFO; (b) frequency dependence of the dielectric constant measured for the PZT ceramic and composite ceramics.

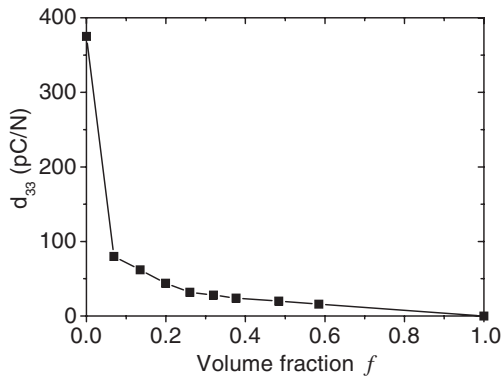


Figure 4. Dependence of the piezoelectric constant d_{33} for the particulate composite ceramics on the volume fraction f of NFO.

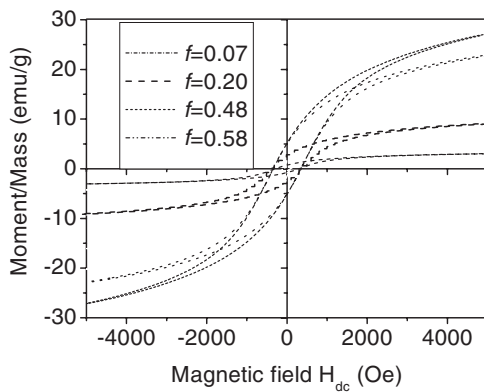


Figure 5. Magnetic hysteresis loops of the composite ceramics.

(figure 3(a)). The large drop (i.e. about 5 times) in d_{33} observed for the composite sample with $f = 0.07$ could be due to the reaction between NFO and PZT when a small amount (e.g. $f = 0.07$) of NFO was added to PZT as discussed above. The introduction of a small amount of NFO into PZT leads to a weakening of the piezoelectric properties of PZT, due to solid solution of Fe and/or Ni in PZT. At high concentrations (e.g. above $f = 0.5$) it is hard to pole the composites, and thus the effective piezoelectric constant of the composites disappears, since the NFO phase with low electrical resistance dominates the properties of the composites with high concentration of NFO.

3.3. Magnetic and ME properties

Figure 5 shows room-temperature hysteresis loops of the NFO/PZT particulate composite ceramics. As expected, it can be seen that the magnetization (and remanent magnetization) of the composites increases and the saturation shifts towards high fields with increase in the volume fraction f of NFO.

We defined $\alpha_{E33}(=dE_3/dH_3)$ as the ME voltage coefficient when the polarization direction (i.e. x_3 -direction) of the sample is parallel to the applied magnetic field. A typical ME hysteresis loop for the NFO/PZT composites is shown in figure 6. The ME hysteresis loop is due to the magnetic hysteresis loop. α_{E33} non-monotonically depends on the magnetic field, with a peak (figures 6 and 7(a)) appearing around 1 kOe. At high magnetic fields, the magnetostriction

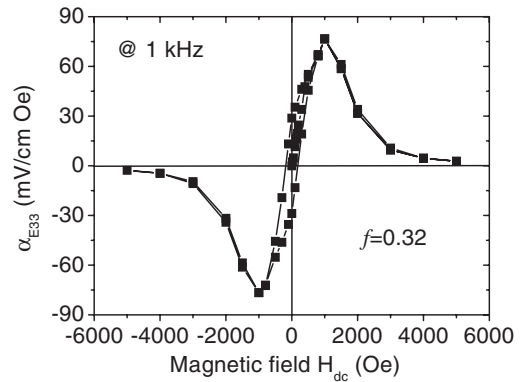


Figure 6. A typical ME hysteresis loop for the composite ceramics.

gets saturated producing a nearly constant electric field in the PZT, thereby causing a decrease in α_{E33} with increase in the magnetic field [24]. In particular, the low magnetic field, α_{E33} shows a good linearity between α_{E33} and the applied magnetic field (figure 7(b)). This behaviour is quite similar to that for the ME devices made from PZT and Ni [4, 5], but the NFO/PZT composite ceramics have higher low-field ME sensitivity than the Ni/PZT devices (i.e. their ME sensitivity of around $1 \text{ mV cm}^{-1} \text{ Oe}^{-1}$). In addition, the composites also illustrates a good linear variation in the ME response with low ac magnetic field (figure 7(c)). Thus, such simple composite ceramics exhibit a large ME response linearly varying with both dc and ac magnetic fields in the low magnetic field range, which potentially makes such simple ceramics attractive for technological applications for the ME devices.

The maximum α_{E33} also depends non-monotonically on the volume fraction f of NFO with a peak (figure 8), as expected, since the ME effect is a product property between piezoelectricity and magnetostriction. With increasing f , α_{E33} increases in the low f range (e.g. $f < 0.32$). This increase is attributed to the increase in magnetostrictively induced strain of the composites with the volume fraction f of NFO. However, with further increase in f , α_{E33} declines after a maximum value, though the magnetostrictively induced strain of the composites still increases with f . This drop in α_{E33} with f is due to a high concentration of the low resistance NFO phase, which can make it difficult to polarize the composites, resulting in a low piezoelectric constant, and, on the other hand, cause the charges developed in the PZT phase to leak through this comparatively low resistance phase path.

The ME coefficient of the NFO/PZT composites is also dependent of the angle θ between the polarization direction (i.e. also the ME voltage measurement direction) and the magnetic field direction. Figure 9 shows a typical example for the NFO/PZT composite with $f = 0.32$. It shows that the α_{E33} value decreases with θ . When the polarization is parallel to the applied magnetic field, i.e. when $\theta = 0$, the α_{E33} value is maximum, but it becomes very low around $\theta = 50^\circ$ – 60° .

In order to understand the ME anisotropy shown in figure 9, let us consider a simple model as shown in figure 10. Unit cell 1 denotes the magnetostrictive phase, NFO, and unit cells 2–4 denote the piezoelectric phase, PZT. First we investigate the charge generated in unit cell 3. When the polarization direction is parallel to the magnetic field

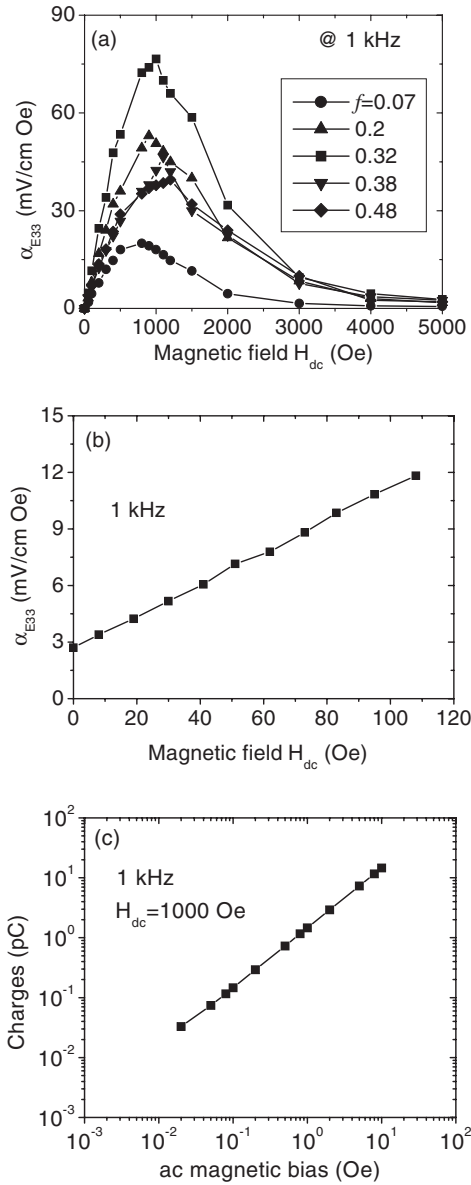


Figure 7. (a) Magnetic-field-dependent α_{E33} of the composites with various NFO volume fractions f ; (b) a low-field ME response of the composite with $f = 0.32$; (c) induced ME charges as a function of the ac magnetic field measured for the composite with $f = 0.32$.

(figure 10(b)), then the charges Q can be expressed as

$$Q \propto S \times (\lambda_{33} \times e_{33} + \lambda_{31} \times e_{31} + \lambda_{32} \times e_{31}) \quad (1)$$

where S is the area of the interface between the cubic unit cells 1 and 3, e_{33} and e_{31} are piezoelectric constants, λ_{33} is the magnetostriction parallel to the magnetic field, and λ_{31} and λ_{32} are the magnetostriction perpendicular to the magnetic field. When the polarization direction has an angle θ with respect to the magnetic field (figure 10(c)), equation (1) is rewritten as

$$Q \propto S \times (\lambda'_{33} \times e_{33} + \lambda'_{31} \times e_{31} + \lambda'_{32} \times e_{31}) \quad (2)$$

where λ'_{ij} are the magnetostrictive strains along the x'_i axes, and are related to λ_{ij} by the matrix transforming the new axes

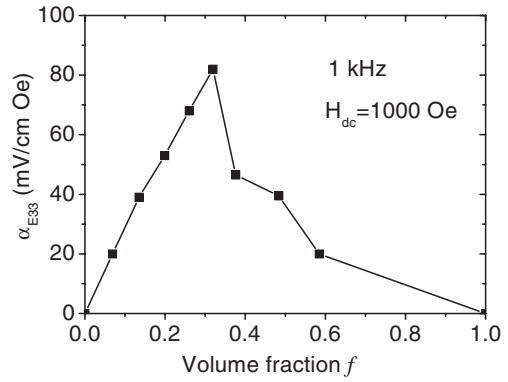


Figure 8. Dependence of α_{E33} at 1 kOe and 1 kHz for the particulate composite ceramics on the volume fraction f of NFO.

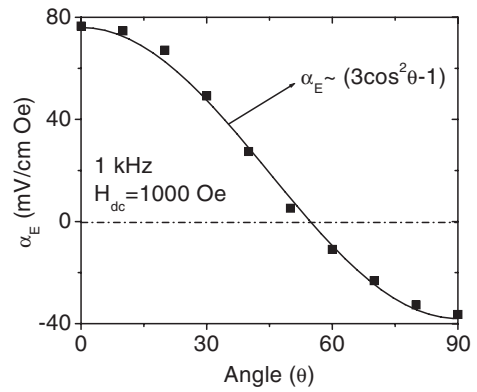


Figure 9. Variation of the ME voltage coefficient with angle θ between the magnetic field H_{dc} and the polarization, measured for the composite with $f = 0.32$. The solid line corresponds to equation (6).

x'_i for any θ to the old axes x_i for $\theta = 0^\circ$, namely,

$$\lambda'_{ij} = \sum_{k,l} a_{ik} a_{jl} \lambda_{kl} \quad (3)$$

where a_{ik} are the direction cosines between x'_i and x_k . Furthermore, in the present case, when the sample is rotated along the x_2 -axis (figure 10(c)) and the magnetic field along the x_3 -axis, equation (3) reduces to

$$\begin{aligned} \lambda'_{31} &= \cos^2 \theta \lambda_{31} + \sin^2 \theta \lambda_{33} \\ \lambda'_{32} &= \lambda_{32} \end{aligned} \quad (4)$$

$$\lambda'_{33} = \sin^2 \theta \lambda_{31} + \cos^2 \theta \lambda_{33}$$

Thus, from equations (2) and (4), we obtain

$$Q \propto S \times [(\sin^2 \theta \lambda_{31} + \cos^2 \theta \lambda_{33}) \times e_{33} + (\cos^2 \theta \lambda_{31} + \sin^2 \theta \lambda_{33}) \times e_{31} + \lambda_{31} \times e_{31}] \quad (5)$$

The same results can be obtained from unit cells 2 and 4. For cubic NFO, after saturation, $\lambda_{33} \approx -2\lambda_{31}$ and $\lambda_{31} = \lambda_{32}$, equation (5) becomes

$$Q \propto S \times (3 \cos^2 \theta - 1) \times \lambda_{31} \times (e_{31} - e_{33}) \propto 3 \cos^2 \theta - 1 \quad (6)$$

which means that the total charges generated in the composites, i.e. the ME coefficient, is proportional to $3 \cos^2 \theta - 1$. Figure 9 shows the behaviour observed in the experiment.

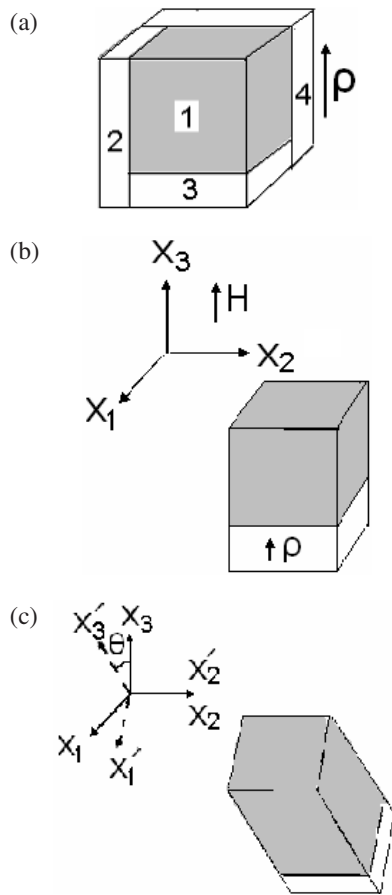


Figure 10. (a) Schematic diagram of a cube model; (b) and (c) schematic illustration of the magnetic field H_{dc} with respect to the polarization direction.

4. Conclusions

The simple particulate composites of NFO/PZT were fabricated by conventional ceramic processing. The ME effect of the bi-ferroic composites is strongly dependent on the volume fraction f of NFO. A maximum ME effect of about $80 \text{ mV cm}^{-1} \text{ Oe}^{-1}$ has been observed in the composite with $f = 0.32$. The dependence of the ME response of the composites on the applied magnetic fields and the ME anisotropy are dominated by NFO. In particular, the simple composite ceramics exhibit a very large ME response linearly varying with both dc and ac magnetic fields in the low

field range, which makes such simple ceramics attractive for technological applications for ME devices.

Acknowledgments

This work was supported by the NSFC under grant 50232030 and 50172026, the Ministry of Sciences and Technology of China through 973-Plan under grant 2002CB613303, and Tsinghua Foundation.

References

- [1] Bichurin M I (ed) 2002 *Proc. 4th Int. Conf. on Magnetolectric Interaction Phenomena in Crystals MEIPIC-4, Ferroelectrics* **282** 1
- [2] Shin K H, Inoue M and Arai K I 2000 *Smart Mater. Struct.* **9** 357
- [3] Wolf S A, Awschalom D D and Buhrman R A 2001 *Science* **294** 1488
- [4] Peto J L, Aroca C, Lopze E, Sanchez M C and Sanchez P 1996 *J. Appl. Phys.* **79** 7099
- [5] Michelena M D, Montero F and Sanchez P 2002 *J. Magn. Mater.* **242** 1160
- [6] Astrov D N 1961 *Sov. Phys.—JETP* **13** 729
- [7] Rado G T and Folen V J 1961 *Phys. Rev. Lett.* **7** 310
- [8] VanRun A M J G, Terrell D R and Scholing J H 1974 *J. Mater. Sci.* **9** 1710
- [9] Harshe G 1991 *PhD Thesis* Pennsylvania State University
- [10] Nan C-W 1994 *Phys. Rev. B* **50** 6082
- [11] Lopatin S, Lopatin I and Lisnevskaya I 1994 *Ferroelectrics* **162** 63
- [12] Bichurin M I, Kornev I A, Petrov V M and Lisnevskaya I 1997 *Ferroelectrics* **204** 289
- [13] Patankar K K and Domebale P D 2001 *Mater. Sci. Eng. B* **87** 53
- [14] Ryu J, Carazo A V, Uchino K and Kim H E 2001 *J. Electroceram.* **7** 17
- [15] Srinivasan G, Rasmussen E T, Levin B J and Hayes R 2002 *Phys. Rev. B* **65** 134402
- [16] Kim J S, Cheon C II, Choi Y M and Jang P W 2003 *J. Appl. Phys.* **93** 9263
- [17] Zhai J Y, Cai N, Liu L, Lin Y H and Nan C W 2003 *Mater. Sci. Eng. B* **99** 329
- [18] Getman I 1994 *Ferroelectrics* **162** 45
- [19] Benveniste Y 1995 *Phys. Rev. B* **51** 16494
- [20] Li J and Dunn M L 1998 *Philos. Mag. A* **77** 1341
- [21] Huang J H 1998 *Phys. Rev. B* **58** 12
- [22] Bichurin M I, Petrov V M and Srinivasan G 2002 *J. Appl. Phys.* **92** 7681
- [23] Ikeda T 1984 *Fundamental of Piezoelectric Materials* (Tokyo: Ohm Publication)
- [24] Nan C-W, Li M and Huang J H 2001 *Phys. Rev. B* **63** 144415